Investigation of the intrinsic magnetic properties of GdCo4B single crystal: determination of the magnetocrystalline anisotropy from the first-order magnetization processes

V. Svitlyk, M. Kuz'min, Y. Mozharivskyj, O. Isnard

Investigation of the intrinsic magnetic properties of $GdCo_4B$ single crystal: determination of the magnetocrystalline anisotropy from the first-order magnetization processes

V. Svitlyk[1,2], M.D. Kuz'min[3], Y. Mozharivskyj [4], O. Isnard[5]

[1]*Helmholtz-Zentrum Dresden-Rossendorf, Institute of Resource Ecology, 01314 Dresden, Germany*

[2]*Rossendorf Beamline (BM20), European Synchrotron Radiation Facility, 38043 Grenoble, France*

[3]*Aix-Marseille Université, IM2NP, UMR CNRS 7334, F-13397 Marseille Cédex 20, France*

[4]*Department of Chemistry and Chemical Biology, McMaster University, 1280 Main Street West, Hamilton, Ontario, Canada*

[5]*Université Grenoble Alpes, Institut Néel, CNRS, BP166X, 38042 Grenoble Cédex 9, France*

svitlyk@esrf.fr michael.kuzmin@univ-amu.fr
mozhar@mcmaster.ca olivier.isnard@neel.cnrs.fr

Abstract

We report on the intrinsic magnetic properties of a $GdCo_4B$ single crystal as derived from magnetization measurements. The occurrence of a first-order magnetization process (FOMP) in a magnetic field applied perpendicularly to the easy magnetization direction provides a unique opportunity to determine the anisotropy parameters K_1 and K_2. To this end, the theoretical approach proposed previously for easy-plane magnets has been adapted for the case of easy-axis compounds exhibiting a FOMP. The obtained anisotropy parameters of $GdCo_4B$ are successfully compared with the values deduced by other classical techniques. The presence of a compensation point in the thermal dependence of the spontaneous magnetization has enabled the determination of the exchange field on Gd, B_{ex} = 129 T, which is in good agreement with inelastic neutron scattering results published earlier. Influence of the applied pressure on the anisotropy parameters is quantified using the pressure dependence of the FOMP, revealing a significant sensitivity of the anisotropy parameters to pressure.

Keywords: rare-earth transition metal intermetallics, X-ray diffraction, crystal structure, magnetic phase diagram, magnetic anisotropy constant

1. Introduction

It is generally possible to substitute boron for cobalt in RCo_5 to obtain the compounds $R_{n+1}Co_{3n+5}B_{2n}$, n =0, 1, 2, 3, ∞, which form a unique series of crystal structures changing with n [1–5]. All these structures are derived from the $CaCu_5$-type structure and differ in the ordering scheme of the B for Co substitution in RCo_5. RCo_4B compounds have been widely studied, first for their crystal structure and later because of their interesting physical properties [4,6,7]. A special interest in the magnetic properties results from the combination of rare-earth and transition-metal sublattices, which provide localized and itinerant magnetism, respectively.

The $GdCo_4B$ compound has been reported to crystallize in the $CeCo_4B$-type crystal structure, obtained by an ordered substitution of B for Co on the 2*c* Wyckoff positions, thus leading to a doubling of the unit cell along the hexagonal *c* axis. The *P*6/*mmm* space group is retained. The $GdCo_4B$ compound has attracted much attention from a fundamental point of view. It was first investigated on polycrystalline samples [3,4,6–10], later a single crystal was produced [11,12]. The crystal structure was determined from an X-ray study of a single crystal [13]. The magnetic properties have been investigated by a number of research teams and techniques, ranging from magnetization measurements [3,4,7,10] through nuclear magnetic resonance spectroscopy [14] to high magnetic field studies [15,16] and X-ray photoemission spectroscopy [17]. Pressure dependence of the magnetization curves has been explored as well [18,19]. More recently, high-energy neutron scattering experiments and density functional calculations have been performed, aimed at the exchange interactions in $GdCo_4B$ [8].

A remarkable feature of $GdCo_4B$ is that it exhibits a first-order magnetization process when a magnetic field is applied perpendicularly to the six-fold symmetry axis. Another unusual feature of this compound is its easy-axis magnetic anisotropy. This is quite distinct from the behavior of the isotypic YCo_4B compound, which exhibits a spin reorientation at T_{sr} = 155 K [11,19,20], the anisotropy being of the easy-plane type below that point and of the easy-axis type above it. The stronger positive anisotropy of $GdCo_4B$ has been attributed to the Gd sublattice, which is rather unusual for Gd. Generally Gd atoms are not expected to contribute to magnetocrystalline anisotropy, because their half-filled 4f shell has no orbital moment.

In this work we will first investigate the crystal structure of GdCo4B by X-ray diffraction and then focus on the study of its magnetocrystalline anisotropy. In order to extract the anisotropy parameters of the $GdCo_4B$ single crystal in the presence of a first-order magnetization process, we will extend the model previously proposed for magnets with an easy-plane anisotropy to the

case of an easy-axis compound $GdCo_4B$. Then temperature evolution of the anisotropy parameters and their pressure dependence will be determined.

2: Experimental

Single crystal of $GdCo_4B$ was grown using the Czochralski method. An initial polycrystalline $GdCo_4B$ sample was produced by arc-melting of a mixture of Gd (99.9%, CERAC Inc.), Co (99.8%, CERAC Inc.) and B elements (99.9%, Alfa Aesar). The obtained ingot was then placed in a tri-arc furnace on a water-cooled rotating copper hearth. It was subsequently melted with three electric arcs, which guaranteed homogeneity of the melt. Tungsten needle was used as a seed and a 10 mm long $GdCo_4B$ crystal was successfully obtained.

Composition of the obtained sample was verified with a scanning electron microscopy (SEM) technique using a JEOL JSM 7000F microscope. For the SEM analysis, a part of the grown monocrystalline sample was cut off, polished, and subsequently deposited on a carbon tape. The SEM data were normalized using spectra of the stoichiometric $GdCo_5$ compound and the sample under study was found to feature the targeted Gd:Co ratio of 1:4 within the experimental error range. No secondary phases/inclusions were observed. Content of light B atoms was verified using monocrystalline synchrotron radiation diffraction experiment. For this a chipped $GdCo_4B$ single crystal with a size of ca. $150\times150\times150$ μm^3 was mounted on a glass pin. Data were collected on the Swiss-Norwegian beamlines BM01A at the ESRF synchrotron (Grenoble, France) using a KUMA6 diffractometer equipped with the TITAN CCD detector (62 μm pixel size) and a combination of ω- and φ-scans in 1˚ steps. The wavelength of the synchrotron radiation was set to 0.6987 Å. The experimental data were reduced using the CrysalisPro package [21] and refined with the SHELXL software [22].

The isothermal magnetization measurements have been undertaken on a single crystal sample in a wide temperature range from 2 K to 300 K. The measurements have been carried out using the extraction magnetometer at the Néel Institute; the equipment employed has been described elsewhere [23]. In order to determine the ordering temperature and the compensation temperature, isofield magnetization measurements have been recorded above room temperature up to T = 650 K on a SQUID Quantum design ® apparatus.

3: Single crystal diffraction

The synchrotron radiation diffraction data has been analyzed in the *P*6/*mmm* space group, in excellent agreement with earlier reports [7,11,13]. 7619 Bragg reflections with $-9 \le h \le 9$, $-9 \le k \le 9$, $-14 \le l \le 14$ have been collected, and the refinement was done against 336 independent reflections for 15 refined parameters. Summary of the structural refinement for $GdCo_4B$ is presented in Table 1. The refinement led to a Goodness-of-fit on F^2 of 1.138 and final agreement factors of $R_1 = 0.0372$, $wR_2 = 0.1017$. All atomic sites, including that of B, were found to be fully occupied. We therefore conclude that the crystal studied in this work is of targeted $GdCo_4B$ composition and without secondary phases. The lattice parameters obtained at room temperature are as follows: $a = 5.0970(3)$ Å, $c = 6.9512(4)$ Å, $\alpha = \beta = 90°$, $\gamma = 120°$. This yields a cell volume of 156.39(2) Å^3 and a density of 8.574 g/cm^3.

The crystal structure obtained is shown in Figure 1, it confirms the ordered substitution of B for Co and the consequent doubling of the unit cell as compared with the $GdCo_5$ structure. The Co atoms in the 6*i* Wyckoff positions are located at $z = 0.2874$, indicating that this atomic plane is closer to the plane containing Gd2 atoms than to the one containing Gd1. The atomic coordinates are in excellent agreement with those reported earlier by Cordier et al. [13]. It is worth to note that anisotropic atomic displacement parameters have been determined. The refined values are essentially equivalent along the U_{11} and U_{33} directions, U_{12} being much smaller for all atomic positions. The Gd1 atoms on the 1*a* site exhibit larger U_{11} values than Gd2 on the 1*b* site. The obtained U_{ii} values are rather close for B and Co2 atoms, but slightly larger values are found for Co1, in particular as regards U_{11} and U_{22} .

Table 1. Crystal data and structure refinement of $GdCo_4B$ single crystal, *P*6/*mmm*, $a = 5.0970(3)$ Å, $c = 6.9512(4)$ Å, V = 156.39(2) Å^3, $R_1 = 0.0372$ for data with $I > 4\sigma(I)$ and $R_1 = 0.0390$ for all data. $U_{23} = U_{13} = 0$ Å^2 for all atoms.

Atom	Site	Occ.	*x/a*	*y/b*	*z/c*	U_{11}, Å^2	U_{22}, Å^2	U_{33}, Å^2	U_{12}, Å^2
Gd1	1*a*	1	0	0	0	0.0182(2)	0.0182(2)	0.0153(2)	0.00912(9)
Gd2	1*b*	1	0	0	½	0.0152(2)	0.0152(2)	0.0138(2)	0.00758(9)
Co1	2*c*	1	⅓	⅔	0	0.0223(4)	0.0223(4)	0.0132(4)	0.0112(2)
Co2	6*i*	1	½	0	0.2874(1)	0.0154(2)	0.0140(3)	0.0152(3)	0.0070(1)
B	2*d*	1	⅓	⅔	½	0.016(2)	0.016(2)	0.014(2)	0.008(1)

A typical Laue diffraction pattern is presented in Figure 2 in order to illustrate the quality of the crystal. The observed Bragg peaks (in black on the film) are compared with the expected ones as derived from calculation (in red). A few Miller indexes are given. This Laue diffraction pattern has been recorded using a polychromatic beam in back scattered geometry

from a tungsten anode X-ray tube. Figure 2 clearly confirms the hexagonal symmetry along the *c* axis in good agreement with the crystal structure derived above.

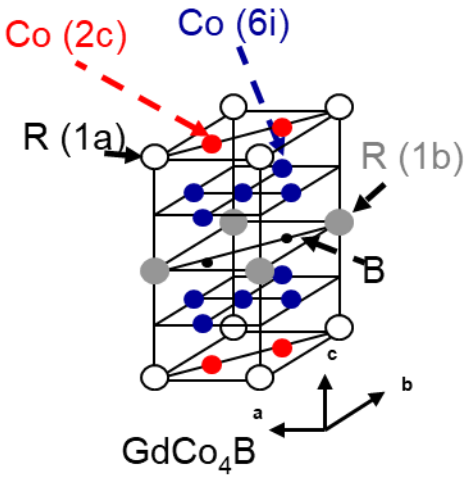

Figure 1 : Schematic diagram of the $GdCo_4B$ crystal structure as derived from single crystal diffraction

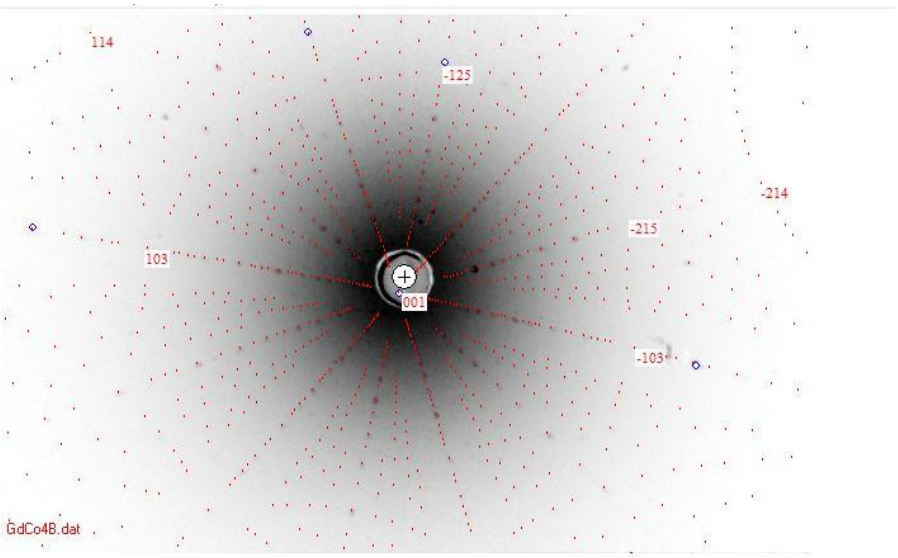

Figure 2: Laue diffraction pattern recorded on the $GdCo_4B$ single crystal with a tungsten anode.

4. Magnetic results and discussion

4.1. Magnetization measurements

As can be seen from Figure 3, the evolution of the low field (0.01 T) magnetization shows two interesting features typical of the ferrimagnetic ordering in $GdCo_4B$. The first one is the compensation temperature, where the magnetization is a minimum since the Gd and Co

sublattices cancel each other out. This occurs at a temperature of T_{comp} = 464 K and low field of 0.01 T was used to demonstrate the negative magnetization around the compensation point. Then at higher temperatures, one can see the transition from the ordered ferrimagnetic state to the paramagnetic state at a Curie temperature of T_C = 564 K. Slightly different values may have been reported in the literature [4,6,10], however, the present values have been determined on a stoichiometric $GdCo_4B$ single crystal and can be regarded as intrinsic values.

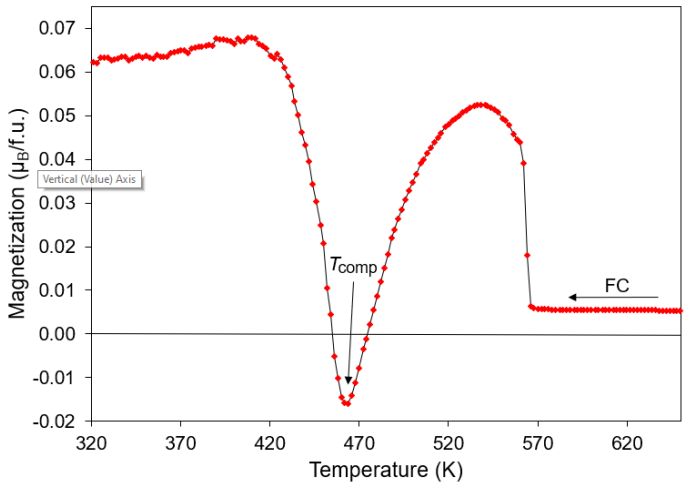

Figure 3 : Thermal evolution of the magnetization of $GdCo_4B$ in an applied field of 0.01 T.

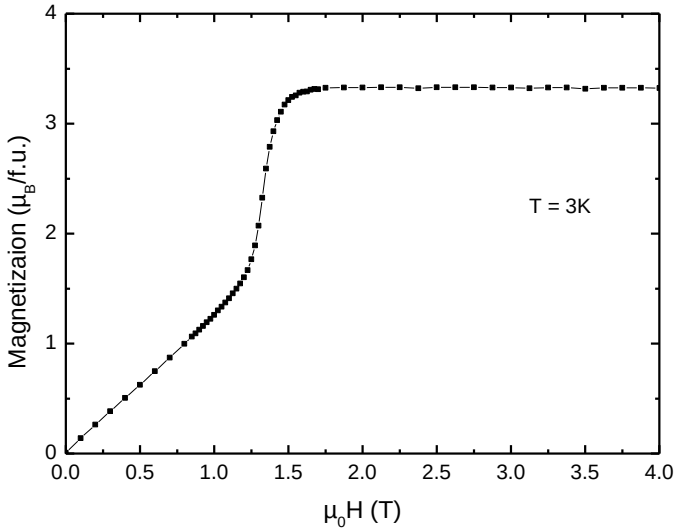

Figure 4 : Isothermal magnetization curve along the *b* axis of $GdCo_4B$ recorded at T = 3 K.

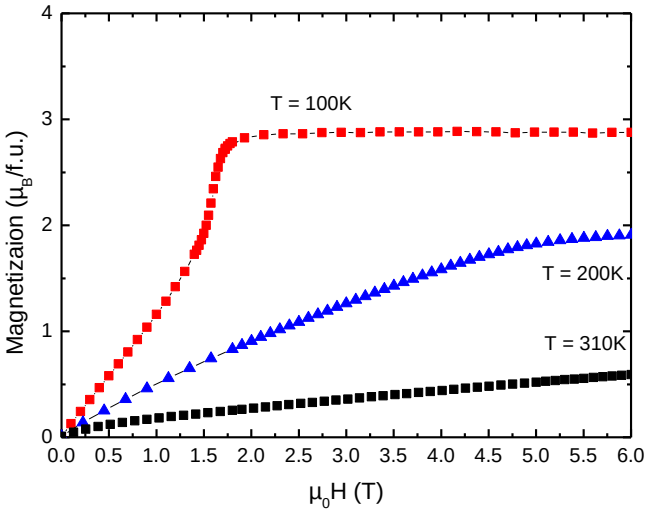

Figure 5 : Comparison of the magnetization curves along the *b* axis of $GdCo_4B$ recorded at T = 100, 200 and 310 K.

The spontaneous magnetization reported by Thang et al. [11] for a single crystal is 3.36 μ_B/f.u. at T = 5 K, a value close to 3.25 μ_B/f.u. derived by Burzo et al. [4]. Here, we obtain a similar value of 3.33 μ_B/f.u. by extrapolation of the saturated part of the magnetization curve to zero field (see Figure 4). Thang et al. [11] showed that the easy magnetization direction in $GdCo_4B$ is the *c* axis and reported a first-order magnetization process (FOMP) in the magnetization curves recorded along the *b* axis. Such a feature is also present in our magnetization curves (see Figure 5) taken at the low temperatures; it disappears progressively as the temperature is raised.

4.2. Determination of anisotropy parameters from a first-order magnetization process

The anisotropy energy of a uniaxial crystal is written as follows:

$$E_a = K_1 \sin^2\theta + K_2 \sin^4\theta, \qquad (1)$$

where K_1 and K_1 are anisotropy parameters, often called anisotropy constants even though they depend on temperature. Below we shall determine these parameters for $GdCo_4B$ as functions of temperature using a new approach.

Indeed, at low temperatures the $GdCo_4B$ magnetization curves recorded along the hard direction ($\boldsymbol{H}\perp[001]$) have an anomaly (a jump) characteristic of a first-order reorientation transition (FOMP). According to Asti and Bolzoni [24,25], this FOMP is of type I: the jump begins at certain critical magnetization and magnetic field, M_{cr} and H_{cr}, and ends in a state of

technical saturation, $M = M_s$, M_s being the spontaneous magnetization. In this case the standard Sucksmith-Thompson technique [27] is inefficient because only a small initial portion of the magnetization curve – well below the FOMP anomaly – can be used for the determination of K_1 and K_2. In an earlier work on Tb_2Fe_{17} [26], it was proposed to express K_1 and K_2 directly in terms of M_{cr} and H_{cr} (as well as $m_{cr} = M_{cr}/M_s$). Unlike Tb_2Fe_{17}, $GdCo_4B$ is an easy-axis magnet, therefore, the equations derived in Ref. [26] have to be modified accordingly. The modification concerns only the expression for K_1, which now becomes

$$K_1 = \frac{1+2m_{cr}+3m_{cr}^2}{2m_{cr}(1+m_{cr})^2}\mu_0 M_s H_{cr}\,, \qquad (2)$$

whereas the formula for K_2 remains unchanged,

$$K_2 = -\frac{\mu_0 M_s H_{cr}}{2m_{cr}(1+m_{cr})^2}\,. \qquad (3)$$

Equations (2) and (3) were used to process the magnetization curves taken at $T \leq 100$ K, where the FOMP is clearly visible. The so-obtained values of K_1 and K_2 are plotted against T in Figure 6, and the values are listed in Table 2 for some temperatures. At $T \geq 100$ K, K_1 and K_2 were determined by the usual Sucksmith-Thompson technique [27] and the values obtained by both methods match at $T = 100$ K (Figure 6).

Table 2: Experimental values of K_1 and K_2 of $GdCo_4B$ derived from the FOMP by using Eqs. (2, 3).

T (K)	K_1 (J/Kg) @0kbar	K_2 (J/Kg) @0kbar
2	60.3	-21.9
30	53.1	-18.3
90	49.8	-13.7
100	51.4	-13.3

Turning now to the thermal dependence of the spontaneous magnetization of $GdCo_4B$, this can be presented as follows:

$$M_s(T) = 7\mu_B B_{7/2}\left(\frac{7\mu_B B_{ex} f(T/T_C)}{kT}\right) - M_{Co}(0)\, f(T/T_C). \qquad (4)$$

Here $B_{7/2}(x)$ is the Brillouin function for $J = 7/2$, B_{ex} is the exchange field on Gd produced by the Co sublattice, and $M_{Co}(0) = 3.67$ μ_B/f.u. is the Co sublattice moment at T=0, chosen so as to reproduce the spontaneous magnetization measured at low temperatures, $M_s(0) = 3.33$ μ_B/f.u. Further, $f(T/T_C)$ stands for a function describing the thermal dependence of the Co sublattice magnetization [28,29]:

$$f(T/T_C) = \left[1 - s(T/T_C)^{3/2} - (1-s)(T/T_C)^{5/2}\right]^{1/3}. \quad (5)$$

The compensation temperature is determined from an obvious condition, $M_s(T_{comp}) = 0$. It should be noted that the resulting value of T_{comp} depends essentially on B_{ex} only. The form of the function $f(T/T_C)$ and the values of the parameters s and T_C have only a minor effect on T_{comp}. By linearizing the Brillouin function, $B_{7/2}(x) \approx \frac{3}{7}x$, one can eliminate the factor $f(T/T_C)$ from the condition for T_{comp}, which then becomes directly proportional

$$kT_{comp} = 21\mu_B^2 M_{Co}^{-1}(0) B_{ex} \quad (6)$$

This relation is however an approximate one. This is because at the compensation point, the argument of the Brillouin function is $x \sim 1$, rather than $x << 1$ as required for the linearization to be accurate. We therefore prefer to use Eqs. (4) and (5) for finding T_{comp}. The value of T_c is then taken from the experiment, while the parameter s is fixed at $s = 0.7$ like in YCo_5 [28]. Firstly, $s = 0.7$ is a value typical for ferromagnets [29]. Secondly, as stated above, varying s rather than having it fixed does not change T_{comp} very much.

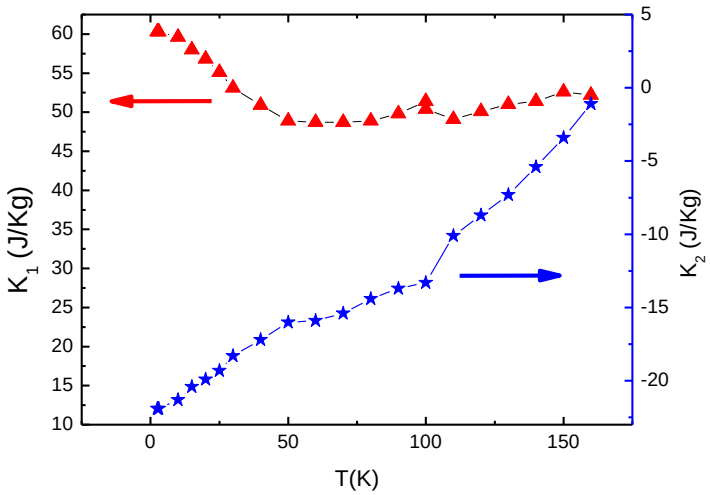

Figure 6: Thermal evolution of the anisotropy parameters K_1 and K_2 of $GdCo_4B$.

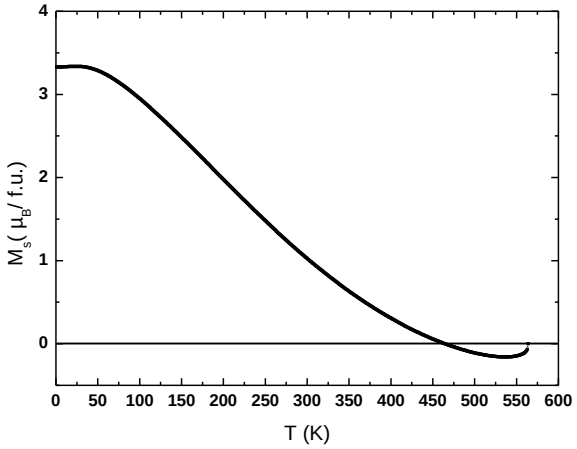

Figure 7: Thermal evolution of the spontaneous magnetization of $GdCo_4B$ found from Eqs. (4, 5) with T_C = 564 K, B_{ex} = 129 T, and s = 0.7.

4.3. Discussion

The values of K_1 and K_2 obtained at T=2 K are 60 and -22 J/kg, respectively. Whereas K_1 changes rather little with temperature, becoming about 52 J/kg at T=155 K, K_2 experiences a much faster decay, from -22 J/kg at T=2 K to practically zero at T=155 K. The anisotropy parameters obtained here from the FOMP are in good agreement with the values found previously by fitting magnetization curves [11]. This validates the theoretical approach described above and provides a new method to determine the magnetocrystalline anisotropy parameters in compounds exhibiting a FOMP.

Z. Arnold et al. have reported the pressure dependence of the magnetization curves for a $GdCo_4B$ single crystal [19]. Their study revealed that the FOMP observed for $GdCo_4B$ is highly sensitive to the application of external pressure to the compound. We used the experimental data of Ref. [19] to derive the anisotropy parameters by the method described in the previous section; those data had been recorded at different pressures but under the same conditions and in the identical pressure cell [19]. From the 30 K data set of Ref. [19], we deduced K_1=64 J/kg and K_2=-25.6 J/kg at P=6.1 kbar, as well as K_1=61.6 J/kg and K_2=-22.8 J/kg at P=0. The zero-pressure anisotropy parameters are slightly different from those obtained in the previous section, because single crystals of different provenance were used. It is interesting to note that at T=30 K, which is below the minimum in $K_1(T)$ situated at T=60 K, both K_1 and K_2 are strengthened by the pressure. On the contrary, at temperatures above 60 K both K_1 and K_2 are reduced under pressure. Thus, at T=90 K, we got K_1=58.9 J/kg and K_2=-

18.9 J/kg at P=6.5 kbar, as against K_1=59.8 J/kg and K_2=-19.2 J/kg at P=0. At T=30 K the pressure derivatives of the anisotropy parameters are estimated to be $\partial K_1/\partial P$ = 0.41 J kg^{-1} kbar^{-1} and $\partial K_2/\partial P$ = -0.46 J kg^{-1} kbar^{-1}. At T=90 K both derivatives have changed sign and become about three times smaller in magnitude.

Using the characteristic temperatures of our $GdCo_4B$ single crystal, T_{comp} = 464 K and T_C = 564 K, we find from Eqs. (4, 5) an exchange field of B_{ex} = 129 T. This value is in excellent agreement with that obtained from inelastic neutron scattering measurements, 130(10) T [8]. This is a further confirmation of the reliability of the theoretical approach described in the present work. Calculations using smaller values of T_{comp} and T_C, taken from the literature [15,16], yielded a much smaller exchange field. DFT calculations [8] have predicted a significantly larger exchange field on the 1*a* site than on the 1*b* one. This is not surprising if one considers that Gd(1*a*) have 6 more cobalt atoms as nearest neighbors than Gd(1*b*) have. However, only a mean exchange field can be estimated from our experimental studies, corresponding to an average value for the two gadolinium sites. Similarly, the limited resolution of inelastic neutron scattering in Ref. [8] did not allow to distinguish between the two inequivalent Gd positions.

5. Conclusions

A single crystal of $GdCo_4B$ has been synthesized and its crystal structure investigated by X-ray diffraction. Investigation of the magnetic properties has yielded T_{comp} = 464 K and T_C = 564 K for the compensation temperature and the Curie temperature, respectively. Hence the mean exchange field experienced at the Gd atomic positions, B_{ex} = 129 T (at T = 0). At low temperatures, a remarkable first-order magnetic transition occurs when recording the magnetization along the hard magnetization direction. A theoretical model has been developed to access the anisotropy parameters for this kind of FOMP. This approach, employed originally for easy-axis magnetic compounds, is found to perform well for $GdCo_4B$, as judged from the comparison with earlier published results [11]. The method is applicable to both easy-plane and easy-axis materials with a FOMP and is complementary to the well-known Sucksmith-Thomson technique, which is disadvantageous for such materials.

The effect of pressure on the anisotropy parameters K_1 and K_2 has been investigated using the same method and earlier published magnetization curves [19]. The anisotropy of $GdCo_4B$ is found to depend strongly on pressure and temperature.

Acknowledgement: The authors wish to express their gratitude to Jérôme Debray of Institut Néel for assistance with the orientation of the single crystal.

Data Availability Statement: Data supporting the findings of this study are available upon reasonable request.

References

1. Y. B. Kuz'ma and N. S. Bilonizhko, Sov. Phys. Crystallogr. **18(4)**, 447 (1974).

2. Y. B. Kuz'ma, *Crystal Chemistry of Borides* (University of Lviv, Lviv, 1983).

3. A. T. Pedziwiatr, S. Y. Jiang, W. E. Wallace, E. Burzo, and V. Pop, J. Magn. Magn. Mater. **66**, 69 (1987).

4. E. Burzo, I. Creangă, and M. Ursu, Solid State Commun. **64**, 585 (1987).

5. C. Zlotea, C. Chacon, and O. Isnard, J. Appl. Phys. **92**, 7382 (2002).

6. H H A Smit, R C Thiel, and K H J Buschow, J. Phys. F Met. Phys. **18**, 295 (1988).

7. C. Chacon and O. Isnard, J. Solid State Chem. **154**, 242 (2000).

8. O. Isnard, M. D. Kuz'min, M. Richter, M. Loewenhaupt, and R. Bewley, J. Appl. Phys. **104**, 13922 (2008).

9. O. Isnard and C. Chacon Carillo, J. Alloy. Compd. **442**, 22 (2007).

10. Z. Drzazga, J. Magn. Magn. Mater. **89**, 97 (1990).

11. C. V Thang, P. E. Brommer, J. H. P. Colpa, N. P. Thuy, and J. J. M. Franse, Phys. B Condens. Matter **228**, 205 (1996).

12. C. V. Thang, Ph. D. Thesis, University van Amsterdam (Netherlands), 1996.

13. G. Cordier, R. Klemens, and B. Albert, Z. Anorg. Allg. Chem. **633**, 1603 (2007).

14. H. Yoshie, M. Hoshino, Y. Amako, H. Nagai, H. Wada, M. Shiga, and Y. Nakamura, J. Phys. Soc. Japan **64**, 2243 (1995).

15. T. Ito, H. Ogata, H. Ido, and G. Kido, J. Appl. Phys. **73**, 5914 (1993).

16. Y. Suzuki, T. Ito, T. Uchida, O. Nashima, N. M. Hong, and H. Ido, J. Appl. Phys. **81**, 5141 (1997).

17. A. Kowalczyk, G. Chełkowska, and A. Szajek, Solid State Commun. **120**, 407 (2001).

18. J. Kamarád, Z. Arnold, O. Mikulina, V. Sechovský, H. Ido, and N. M. Hong, Phys. B Condens. Matter **237**–**238**, 527 (1997).

19. Z. Arnold, J. Kamarád, Y. Skorokhod, N. M. Hong, N. P. Thuy, and C. V Thang, J. Magn. Magn. Mater. **262**, 382 (2003).

20. H. Mayot, O. Isnard, Z. Arnold, and J. Kamarad, J. Phys. Condens. Matter **20**, 135207 (2008).

21. Rigaku Oxford Diffraction, (2021), CrysAlisPro Software System, Version 1.171.42.37a, Rigaku Corporation, Wroclaw, Poland.

22. G. M. Sheldrick, Acta Cryst. C **71**, 3 (2015).

23. A. Barlet, J. C. Genna, and P. Lethuillier, Cryogenics (Guildf). **31**, 801 (1991).

24. G. Asti and F. Bolzoni, J. Magn. Magn. Mater. **20**, 29 (1980).

25. G. Asti, *First Order Magnetization Processes. Handbook of Magnetic Materials 5, 397* (Elsevier, 1990).

26. M. D. Kuz'min, Y. Skourski, K. P. Skokov, K.-H. Müller, and O. Gutfleisch, Phys. Rev. B **77**, 132411 (2008).

27. W. Sucksmith and J. E. Thompson, Proc. R. Soc. London, Ser. A **225**, 362 (1954).

28. M. D. Kuz'min, Phys. Rev. Lett. **94**, 107204 (2005).

29. M. D. Kuz'min, K. P. Skokov, L. V. B. Diop, I. A. Radulov, and O. Gutfleisch, Eur. Phys. J. Plus **135**, (2020).